

MQP – BIO – DSA – 3046
MQP – BIO – DSA – 8280

**Real-time PCR Study of $\alpha 4\beta 2$ nAChR Gene Expression During Chronic
Nicotine Treatment of H69 Cells**

A Major Qualifying Project Report

Submitted to the Faculty

of the

WORCESTER POLYTECHNIC INSTITUTE

in partial fulfillment of the requirements for the

Degree of Bachelor of Science

in

Biology and Biotechnology

by

Jaime L. Grouf

Stacia L. Richards

April 28, 2005

APPROVED:

Paul D. Gardner, PhD
Department of Psychiatry
Brudnick Neuropsychiatric Research Institute
UMass Medical School
Major Advisor

David S. Adams, PhD
Dept. of Biology and Biotechnology
Worcester Polytechnic Institute
WPI Project Advisor

ABSTRACT

The $\alpha 4\beta 2$ subunits comprise a heteromeric nicotinic acetylcholine receptor (nAChR) subtype. Previous studies of nicotine treatment have shown increased receptor expression, but these studies only investigated gene expression utilizing reverse transcriptase PCR. In this study, we treated the H69 human lung carcinoma cell line with nicotine and observed the effects on gene expression using real-time PCR with the hypothesis that nicotine treatment alters gene expression of $\alpha 4\beta 2$ subunits. The advantages of real-time PCR are that it provides the ability to observe amplification at each cycle as well as the ability to perform quantitative analysis on the data. In analyzing a 4 day 100 μM nicotine treatment of the H69 cell line, a significant increase in gene expression of the $\alpha 4$ subunit was observed after 24 hours. Any change prior to or after 24 hours was not significant. These data are indicative of changes in gene expression observed for short periods of nicotine treatment in contrast to long-term treatment.

TABLE OF CONTENTS

Signature Page	1
Abstract	2
Table of Contents	3
Acknowledgements	4
Background	5
Project Purpose	21
Methods	22
Results	26
Discussion	46
Bibliography	50

ACKNOWLEDGEMENTS

The authors would like to extend their sincerest thanks to Dr. Paul D. Gardner for acceptance into his research laboratory, and without whom our educational experience would not have been a success. Gratitude is also extended to Yuly Fabiola Fuentes Medel for her camaraderie, assistance, and collaboration on this project, and Sarah Binke for her technical support. Lastly, we would like to thank David S. Adams for his project initiation, guidance, and assistance in the technical writing of our report.

BACKGROUND

Nicotine

Nicotine (Figure 1) is the primary active agent extracted from the tobacco plant, *Nicotiana tabacum*. It is the addictive stimulant present in chewing tobacco, cigarettes, and other tobacco-related products (Jain and Murkherjee, 2003). One cigarette is estimated to contain 1-3mg of nicotine, causing a smoker's nicotine blood level to reach between 0.1 to 0.5 μ M immediately after smoking a cigarette (Benhammou *et al*, 2000; Pidoplichko, 1997).

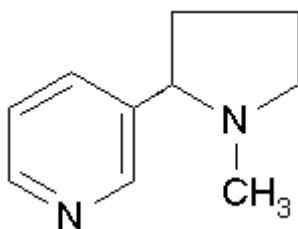


Figure 1: Nicotine Structure. Picture taken from Sigma Aldrich, <http://www.sigmaaldrich.com/>

Addiction to nicotine is characterized by an up-regulation in expression of the nicotinic acetylcholine receptors (nAChRs) in the brain (Benwell *et al*, 1988) and its ability to trigger the release of dopamine, a neurotransmitter that activates the brain's regulation of pleasure sensations, also known as the dopamine reward system (NIDA, 2001). In the human body, a nicotine response is short, fast, and excitatory.

Nicotinic Acetylcholine Receptor

nAChRs (Figure 2) are ligand-gated ion channels involved in cellular modulation and propagation of action potentials ubiquitous throughout the central

nervous system (CNS), peripheral nervous system, and neuromuscular junctions (Dart *et al*, 2000). Among its various agonists are acetylcholine, carbamylcholine and nicotine (Dart *et al*, 2000). nAChRs are pentameric channels structurally assembled from a variety of subunits (α 1- α 10, β 1- β 4, γ , δ , ϵ). Each subunit contains four transmembrane domains (Schapira *et al*, 2002). Neuronal nAChRs are assembled from nine known α (α 2- α 10) and three β subunits (β 2- β 4), either in heteromeric (e.g. α 4 β 2, α 3 β 4, etc.) or homomeric (e.g. α 7) complexes. The receptor's specific subunit composition varies by organ/tissue of the body (Dajas-Bailador and Wonnacott, 2004).



Figure 2: Biochemical Structure of the nAChR in *Torpedo marmorata*.

While the exact composition of the *T. marmorata* nAChR differs from human (α , α , β , γ , δ , ϵ), this picture nonetheless conveys the general structure of the nAChR. Picture obtained from the RCSB protein database (PDB ID# 2BG9) <http://www.rcsb.org/pdb/>

When nicotine binds to the nAChR it induces a receptor conformation change, opening the ion channel for a few milliseconds (Institute of Neurosciences, 2005). This open conformation permits the entry of sodium, potassium or calcium ions into the cell depending upon the ion current and receptor subtype present (Dani *et al*, 2001). If enough

ions enter to surpass a threshold, the cell membrane becomes depolarized, which excites the cell, and propagates an action potential. When the receptor returns to a closed conformation, it is temporarily desensitized to the stimulation of neurotransmitters. Continuous nicotine exposure prolongs this state of desensitization (Institute of Neurosciences, 2005).

nAChR Subunits

As previously mentioned, neuronal nAChRs are pentameric ligand-gated ion channels composed of α and β subunits. The exact combination of subunits depends on the cellular context. In some cases, a specific neuron can express multiple subtypes. Three receptor subtypes are particularly interesting. The $\alpha 4\beta 2$ subtype is the most common receptor found throughout the CNS and is characterized by a high affinity for nicotine. The $\alpha 7$ homomeric receptor is an appealing receptor for research because of its known specific ligand, α -bungarotoxin, which provides an easy tool to study this receptor. Furthermore, the $\alpha 7$ receptor interestingly possesses higher calcium permeability than the NMDA subtype of the glutamate receptors (Séguéla *et al*, 1993). Lastly, while more research is necessary to understand the fundamentals of these specific receptors, far more is known regarding the $\alpha 4\beta 2$ and $\alpha 7$ receptors than any other neuronal subtype.

Neuronal nAChR $\alpha 4\beta 2$ Subtype

The $\alpha 4\beta 2$ subtype (Figure 3) is the most abundant heteromeric nAChR in the central nervous system. Among the numerous types of nAChR, the $\alpha 4\beta 2$ subtype has the

highest affinity for nicotine, constituting greater than ninety percent of nicotine binding in rat brain (Marks *et al*, 1992). The $\alpha 4$ subunit is vital as it specifically interacts with the receptor ligands, nicotine or acetylcholine. The $\beta 2$ subunit contributes structural stability to the receptor subtype as well as reinforcement of nicotine's effects on the nAChR (Marks *et al*, 1992).

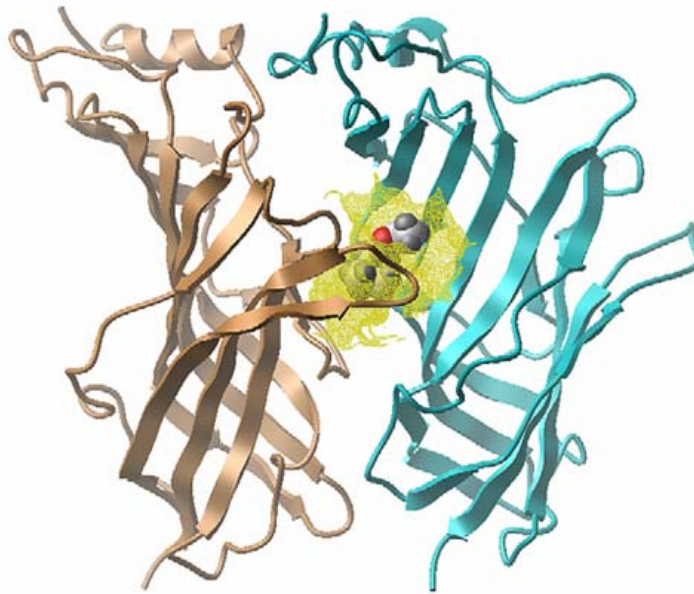


Figure 3: nAChR Type $\alpha 4\beta 2$. Shown here is acetylcholine (yellow), the endogenous ligand of the nAChRs, bound to the ligand binding site of the $\alpha 4$ (left) and $\beta 2$ (right) subunit monomers of the receptor pore. Note that this is only a model of the subunit interaction and the nAChRs are actually pentameric in nature. Picture taken from Schapira *et al*, 2002.

Chronic exposure to nicotine in a dose-dependent manner has consistently demonstrated an up-regulation or increase in nicotinic receptor concentration. In 1992, Marks *et al* established the paradigm that while chronic nicotine treatment does increase the number of nicotine binding sites on the plasma membranes of cells, this effect is not a direct result of up-regulation of the $\alpha 4$ and $\beta 2$ nAChR subunit genes, but post-transcriptional (Marks *et al*, 1992). However, a few other plausible possibilities exist to

explain the observed increase in nicotine binding sites per cell, nicotine may increase the efficiency of receptor incorporation into cellular membranes, it may stabilize the RNA transcript such that it exists in the cytoplasm longer allowing more translation, or nicotine may attenuate the receptor degradation rate (Marks *et al*, 1992). The Marks *et al* (1992) study was validated by Benhammou *et al* (2000) who described a positive correlation between the number of cigarettes smoked each day and the number of nicotine binding sites in human lung tissue.

The potential role of the $\beta 2$ subunit in transmission of nicotine-related responses and behavior was investigated by Picciotto *et al* in 1998. The authors used a $\beta 2$ knockout mouse model and found that the neurons in these mice lacked the ability to elicit a response to nicotine simulation as compared to wild type mice, indicating that the $\beta 2$ subunit is responsible for neurotransmission responses to nicotine. Picciotto *et al* also found that in nicotine self-administration experiments, the knockout mice showed a significant decrease in the number times they would drink from a bottle of water containing nicotine as compared to the wild type, reinforcing the role of this receptor in mediating the effects of nicotine.

Neuronal nAChR $\alpha 7$ Subtype

The $\alpha 7$ subtype is another receptor of the nAChR family that is frequently studied as it is one of the only known nAChR subtypes able to form a homopentameric receptor. While this subunit has a lower affinity for nicotine than the $\alpha 4\beta 2$ subtype, it does possess a high affinity for α -bungarotoxin, and is the predominant protein to bind this toxin in the brain (Peng *et al*, 1997). Specifically, the high affinity for α -

bungarotoxin gives researchers an advantageous tool in studying the $\alpha 7$ receptor. This receptor appears to be involved in numerous physiological processes such as the suppression of apoptosis, learning, memory, schizophrenia, Alzheimer's, inflammation and vasodilation (Severance *et al*, 2004).

In 2004, Trombino *et al* established that nAChR are both expressed and stimulated by nicotine in human mesothelioma cell lines, and that nicotine enhances cell proliferation by binding the $\alpha 7$ receptor. They demonstrated both the ubiquitous presence of $\alpha 7$ subunits throughout these cells as well as calcium ion influx upon stimulation by nicotine binding. It has been previously established that nicotine binding to the $\alpha 7$ nAChR permits the influx of calcium ions, known to activate MAPK signaling cascades which participate in repression of apoptosis. Therefore, Trombino *et al* were able to determine that the calcium ions released by nicotine treatment activated MAPK, which increases the rate of DNA phosphorylation inside the cells, thereby increasing DNA synthesis and inducing elevated rates of cell proliferation.

Peng *et al* (1997) demonstrated that the $\alpha 7$ nAChR receptor subtype is up-regulated by chronic treatment with nicotine, and that this up-regulation and activation only occurs at higher doses of nicotine than is required to upregulate the $\alpha 4\beta 2$ receptor subtype, reaching its maximal up-regulation by 24 hours. Consistent with observations for the $\alpha 4\beta 2$ receptors, no increases of the $\alpha 7$ subunit mRNA were observed, consistent with post-transcriptional regulation.

Nicotine Addiction in Smokers

In smokers, repeated nicotine stimulation increases both the length of time the neuronal membrane is desensitized and the quantity of dopamine released within the brain (Jain and Mukherjee, 2003). Self-administrated reinforcement by nicotine is thought to be regulated in part via the mesolimbic dopamine reward system. Within this system, neuronal projections populated with numerous $\alpha 4$ and $\beta 2$ subunit-comprised nAChRs extend from the ventral tegmental area (VTA) and terminate within the nucleus accumbens (NAc) of the brain (Figure 4). The mesolimbic dopamine projection (orange in the diagram) is an essential component of drug-reinforced behaviors and conditioning associated with substances such as cocaine, heroin, and alcohol. Therefore, nicotinic receptors concentrated in this area function to stimulate dopamine release from dopaminergic neurons thereby reinforcing and propagating both the stimulatory and dependent effects of nicotine (Jain and Mukherjee, 2003).

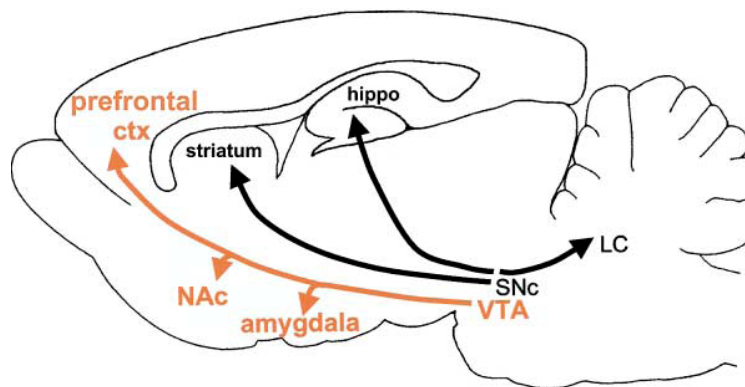


Figure 4: The Mesolimbic Dopamine Projection. Neurons associated with the mesolimbic dopamine reward system (orange in the diagram) project from the ventral tegmental area (VTA) to the nucleus accumbens (NAc) and the prefrontal cortex within the brain. Picture taken from Dani *et al*, 2001.

It is also important to note that nicotine can activate both excitatory dopaminergic neurons and inhibitory GABA neurons within the VTA (Laviolette and van

der Kooy, 2004). These two neuron types play coordinated roles within the VTA. In the early stages of nicotine administration, the inhibitory GABA neurons are predominantly affected and quickly desensitized. This assists in prolonged excitation of dopaminergic neurons as the inhibitory influence of the GABA neurons are temporarily diminished (Laviolette and van der Kooy, 2004).

Contributing to the addictive properties of nicotine is the fact that after depolarization of the neuronal membrane, the endogenous agonist of the AChR, acetylcholine, is easily disposed of by the cell through enzymatic hydrolysis via acetylcholinesterase. Nicotine, on the other hand, can exist for prolonged periods of time at the synapse because it cannot be hydrolyzed by acetylcholinesterase, thus intensifying its desensitizing effects (Dani *et al*, 2001).

During the time between cigarettes, nicotine levels in the blood are high enough to maintain receptor desensitization and pleasure responses (Institute of Neurosciences, 2005). As the nicotine concentration decreases over time, some receptors regain their sensitivity, increasing the levels of acetylcholine neurotransmission which causes agitation and discomfort in the smoker, also known as withdrawal. Ultimately, prolonged receptor desensitization leads to nicotine tolerance and addiction. (Institute of Neurosciences, 2005).

nAChR, Nicotine, and Lung Cancer

Cancer is the second leading cause of death in the United States, second only to heart disease, claiming 557,271 lives in 2002 (American Cancer Society, 2005). Lung cancer is the second leading cause of cancer diagnoses in men and women in the United

States. Unfortunately it is also the primary cause of cancer-related deaths, accounting for approximately 30% of all cancer deaths each year, and expected to kill an estimated 163,510 persons in the year 2005 (American Cancer Society, 2005).

Lung cancers are separated into two main categories: small cell lung carcinomas (SCLC), which are very aggressive lung tumors accounting for 20-25% of all lung cancers, and non-small cell lung carcinomas (NSCLC) (Song *et al*, 2003). Non-small cell lung carcinomas are further subdivided into adenocarcinoma, which is the most prevalent lung cancer in nonsmokers, adenosquamous carcinoma, large cell carcinoma, which comprises 10-15% of lung cancers, and squamous cell carcinoma, the most abundant lung cancer comprising 25-40% of all lung cancers (Song *et al*, 2003).

Small Cell Lung Cancer

Throughout the decades, lung cancer has been linked to the effects of smoking and the carcinogens contained within cigarettes (Song *et al*, 2003). However, researchers have shown that nicotine also may play a role in lung cancer proliferation. In 1993, Cattaneo *et al* provided preliminary data demonstrating the release of serotonin by nicotine-activated AChRs in SCLCs. This was very significant research because serotonin release is tightly coordinated with SCLC growth and proliferation, indicating that nicotine may be a contributing mitogen in tumor growth of the SCLCs.

To further support this study, Mai *et al* in 2003 documented their study displaying nicotine's effect on suppressing apoptosis in SCLC cells, in which they described how nicotine induces phosphorylation of the Bcl2 cellular proto-oncogene

protein, thereby enhancing the *Bcl2* gene function of anti-apoptosis and cell survival within the tumor.

RT-PCR vs. Real-time PCR

This MQP used real-time PCR to monitor levels of nAChR subunit mRNAs in cells treated with nicotine, so we include a brief background on this technique here. With the biotechnology field becoming ever-increasingly complex and analytical, powerful methods for quantifying biological molecules are in high demand. For decades the method of reverse-transcriptase polymerase chain reaction (RT-PCR) has been used to efficiently amplify small quantities of nucleic acids. RT-PCR permits the reverse transcription of RNA into DNA, followed by successive amplification of the template cDNA from a reaction mixture that includes gene-specific primers, dNTP's, and template. However, limitations of this technique include the inability to analyze the target amplified gene of interest (amplicon) at each amplification cycle and the inability to accurately quantify end yields (Lechniak, 2002). When performing RT-PCR, researchers are only able to compare final amplicon yields to a standard on a gel; thus, RT-PCR is only a qualitative technique. In addition to this, variability in reactions and protocols throughout the RT and PCR experiments also make it difficult to accept the quantification results obtained on a gel (Lechniak, 2002). Currently, when using RT-PCR, no technique exists to determine the initial starting concentration of your target nucleic acid. An important problem with traditional RT-PCR is that the same quantity of end product may eventually be formed, even when the starting template concentrations are different.

Real-time PCR is a relatively novel technique that, unlike RT-PCR, can be used to quantify nucleic acid concentrations (Lechniak, 2002). Real-time PCR is an extremely sensitive and powerful technique as it not only can quantify initial sample concentrations, but it allows the researcher to analyze the amplification process at each PCR cycle thus eliminating the need for gel electrophoretic analysis after the reaction, and allowing quantitations to be performed during the exponential phase of the reaction. Theoretically, quantitative real-time PCR can detect products from as few as a single copy of a given sequence (Provanzano *et al*, 2001). This is an extremely sensitive technique compared to alternative gene expression methods.

Real-Time PCR Reporter Dyes

Real-time PCR requires the use of a fluorescent reporter dye to bind to the target and permit detection. These dyes are attached to a probe which also contains a quencher dye so that they only fluoresce upon target binding. Therefore, at each PCR cycle, the amount of product is directly proportional to the light emitted by the dye. Specifically, real-time PCR does not measure the actual nucleic acid amplification, but rather the emitted fluorescence during the reaction. However, in order for the quantification to be valid, the data must be analyzed within the exponential phase of the amplification curve where the reaction occurs at a constant rate.

A few fluorescence reporters exist that can be used to quantify the amplification. Two of the most common dyes are SybrGreen and TaqMan (Lechniak, 2002). Both dyes bind to the minor groove of DNA. SybrGreen is less expensive than

TaqMan but it is less specific as it can also bind to primer dimers and nonspecific products (Lechniak, 2002).

Real-Time PCR Amplification Plot

The exact cycle number at which a significant amount of product will be detected depends upon the initial quantity of the desired target gene. Therefore, higher concentrations of starting material will result in an earlier detection of reporter dye fluorescence and vice versa. Each cycle in real-time PCR increases logarithmically. For example, the amplicon will increase with each cycle 2^1 , 2^2 , 2^3 , 2^4 , and so on, where the exponent is the cycle number (Dorak, 2005).

An amplification plot in real-time PCR (Figure 5) displays the exponential increase of the desired target product. The baseline level is set prior to the log-linear phase and serves as a cut off for background noise. The threshold (green line in the figure), which the operator can manually set, is the point at which a significant increase of fluorescence is detected, typically placed within the exponential phase of the graph. Because it is here that theoretically, all the samples are amplified at the same rate, the researcher can then calculate the amount of starting template in each sample (Figure 5).

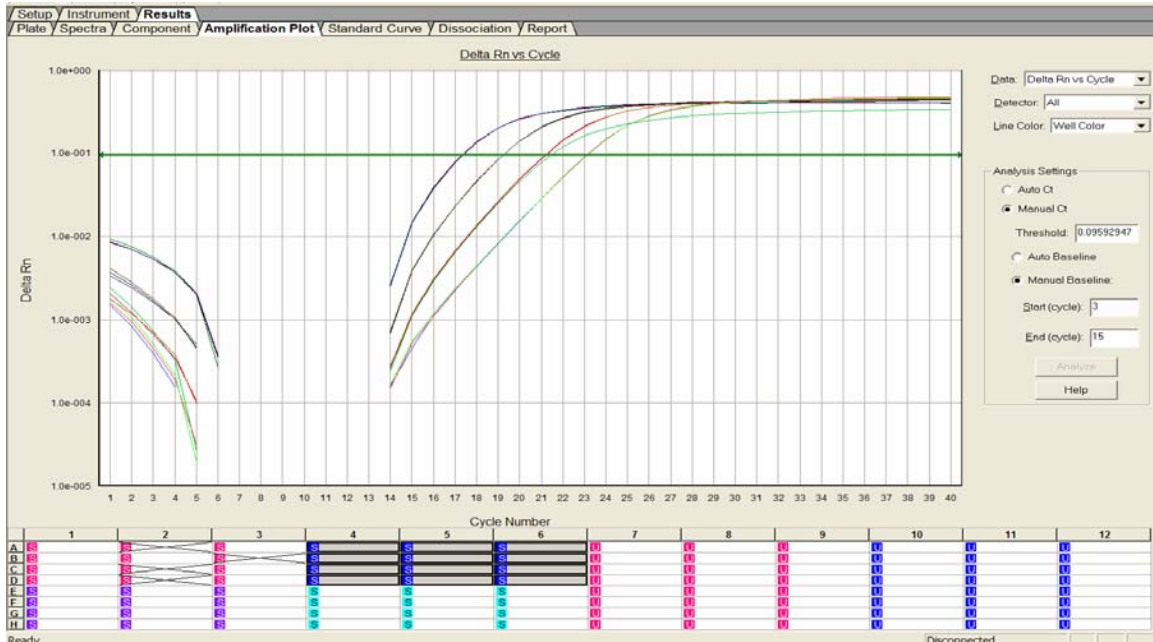


Figure 5: Example of a Real-time PCR Amplification Plot for GAPDH. This plot shows how the threshold (green line) is set where each product is being amplified at approximately the same rate. The 5 reactions shown here differ in dilution. Each dilution has a difference of 2 cycle numbers. Figure taken from Grouf and Richards, 2005.

Real-Time PCR Dissociation Curve

The dissociation curve (Figure 6) is another useful graph that real-time PCR can produce to assist in data analysis. The dissociation curve is also known as a melting curve. This curve provides a method for determining the specificity of the primers. If the plot contains only one peak (as is the case for Figure 6), then it can be inferred that only one target is amplified and the primers are specific to that target. However, if more than one peak appears, the primers may be non-specific. Depending upon the reaction conditions, there may be contamination, primer dimer competition, or non-specific amplification. The dissociation curve also allows one to ensure that the desired amplicon is being detected. This can be determined by comparing the melting temperature at which

the peak is found on the dissociation plot to the assumed melting temperature for the amplicon predicted by the researcher's primer design software (Figure 6).

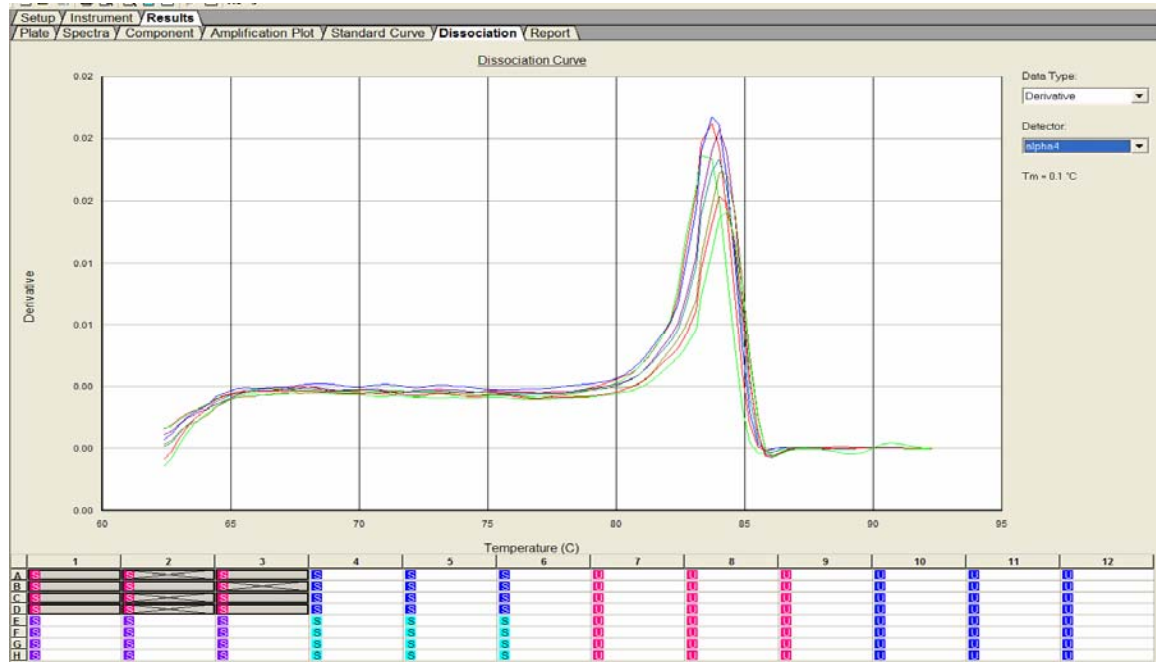


Figure 6: Example of a Real-time PCR Dissociation Curve of the Human nAChR $\alpha 4$ Gene. The $\alpha 4$ AChR primers are specific to the target $\alpha 4$ mRNA. Also 84°C is the correct melting temperature for the desired amplicon. Figure taken from Grouf and Richards, 2005.

Primer Validation

Prior to data analysis, the primers have to be validated. A standard curve (Figure 7) is created for each primer at various concentrations to determine whether or not they have similar reaction efficiencies. For our project, this meant that the primers had to amplify their respective nAChR subunit genes at the same rate (right-side panel in Figure 7), which would permit gene expression to be compared between the subunits and the endogenous control. A standard curve must be created in order to determine that the primers have statistically similar amplification efficiencies. Comparative analysis of the

amplification efficiencies is determined by the slope of the standard curve. A standard curve is made by plotting the cycle (Ct) values on the y-axis versus the log of the dilutions on the x-axis for each primer set. The amplification is a logarithmic increase, therefore, $2^{\text{#cycles}}$ is the exponential increase. A reaction of 100% efficiency will have a slope of -3.33 (Figure 7).

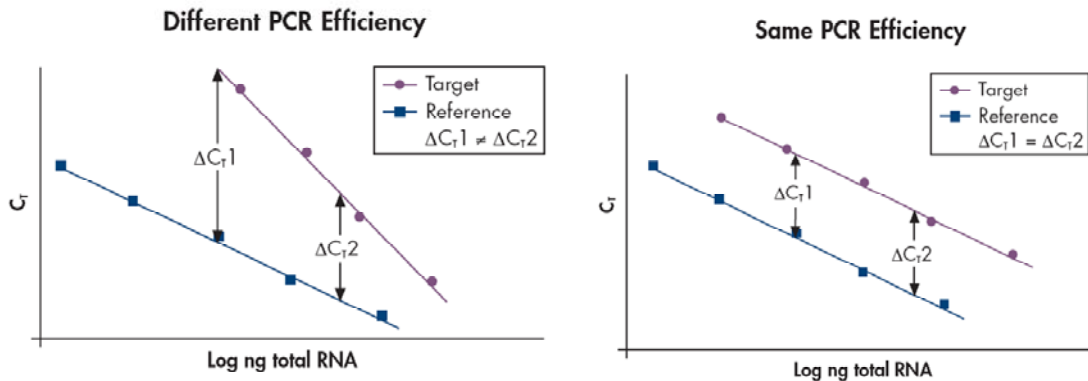


Figure 7: Example Determining PCR Primer Efficiencies.

Validating your primers involves comparing the standard curves of the target gene and the reference, which is typically an endogenous control. The primers need to be amplifying their respective genes at the same rate in order to continue with data analysis. This is achieved by determining the slope of the standard curves and comparing efficiencies. The figure on the left is a typical standard curve showing amplification of two target genes with different PCR efficiencies while the figure on the right shows amplification of two target genes with similar PCR efficiencies. Figure taken from Applied Biosystems.

Significance of the Project

The topic of nicotine effects on nAChRs in the body is of interest because an in-depth understanding of the molecular effects of acute and chronic exposure to nicotine might provide better insight into mechanisms of nicotine addiction, tolerance, and withdrawal. To date, the effects of nicotine treatment on gene expression of the $\alpha 4$, $\alpha 7$

and $\beta 2$ subunits using real-time PCR has not been done. Therefore, in order to provide a more quantitative analysis and in-depth understanding of these molecular interactions, the goal of this project was to use real-time PCR to quantify nAChR gene expression in lung cancer cell lines and to determine if the expression changes in response to nicotine.

PROJECT PURPOSE

The purpose of this study was to quantify changes in the levels of $\alpha 4$ and $\beta 2$ nAChR subunit mRNAs using real-time PCR in H69 and H460 human lung carcinoma cells treated with nicotine for short and long periods of time to test the hypothesis that short-term nicotine treatment increases gene expression of the $\alpha 4$ and $\beta 2$ subunits, while long-term treatment desensitizes the receptor and decreases subunit expression. nAChR gene expression was analyzed using real-time PCR since that method is far more quantitative than traditional RT-PCR, and little work to date has applied this technique to nicotine-treated cancer cells. The cells were treated using a range of nicotine concentrations to determine the optimal dose required to observe an effect on gene expression.

METHODS

Cell Culture

The H69 human small cell lung carcinoma cell line (non-adherent) and H460 human large cell lung carcinoma cell line (adherent) were originally obtained from the American Type Culture Collection (ATCC). Vials were thawed and cultured in RPMI 1640 medium (Gibco) + 10% FBS (HyClone) in the absence of antibiotics. The H69 medium was doubled every other day until maximum flask volume was reached at which point the cells were centrifuged at 1500 rpm for 5 minutes and passaged into new flasks. The H460 cells were cultured to 60% confluency, then trypsinized and passaged using Trypsin-EDTA (Gibco), and centrifuged at 1000 rpm for 5 minutes. Cells were maintained at 37°C in 8% humidified CO₂.

Nicotine Treatment (Dose Response)

H69 and H460 cells were treated with either 1 μM, 10 μM, or 100 μM nicotine (Sigma Aldrich) continuously over a period of seven days. This dose response was performed using duplicate samples in both treatment and control groups. The H69 cells were plated at an initial cell number of 3×10^6 cells, and the H460 cells were plated at an initial cell number of 500,000 cells. The H69 cells were passaged every other day and resuspended in the appropriate medium. Medium was replaced on the H460 cells every other day. Cells were harvested at day seven and stored at -80°C.

Nicotine Treatment (Timed Response)

H69 and H460 cells were treated with 100 μM nicotine for a variety of times over a period of four days. The H69 cells were plated at an initial cell number of 3×10^6 cells, and the H460 cells were plated at an initial cell number of 500,000 cells. As stated before, new medium was supplemented every other day. The cells were harvested at time zero, one hour, 24 hours, and four days.

RNA Isolation

Total cellular RNA was isolated for each sample using a Qiagen RNeasy Midi Kit[®], and the protocol provided by the manufacturer with no exceptions. The assumed starting cell number was a range between a minimum of 5×10^6 cells and a maximum of 1×10^8 cells. Typical yields were approximately 200 μg total, at a concentration of 2 $\mu\text{g}/\mu\text{l}$.

RNA Quantification

Absorbance of total RNA was measured at 260 nm for each sample to calculate the necessary volume to reverse transcribe 2.5 μg of total RNA. RNA was diluted to a concentration of 1/100 prior to quantification. Each absorbance was measured in triplicate. To quantify RNA, the calculation used was as follows:

$$(\text{Average absorbance} \times 40 \times \text{dilution factor}) / 1000 = x \mu\text{g}/\mu\text{L}.$$

$$(2.5 \mu\text{g RNA}) / (x \mu\text{g}/\mu\text{L}) = x \mu\text{L used for Reverse Transcription}.$$

Primer Design

mRNA sequences for nAChR subunits $\alpha 4$, $\alpha 7$, $\beta 2$, and also GAPDH were obtained from GenBank (gi:29570783, gi:21536283, gi:4502832, gi:7669491, respectively). Primers were designed using PrimerExpress[®] software. All primer pairs flanked an intronic sequence to ensure the absence of genomic contamination (determined by electrophoretic analysis). Primers were purchased from Operon Biotechnologies (Huntsville, AL). Lyophilized primers were resuspended in Buffer TE, pH 7.0 to a concentration of 200 μ M, and stored at -20°C.

Reverse Transcription

Using the protocol provided by Ambion, 2.5 μ g of total cellular RNA were reverse transcribed into cDNA for each sample. The calculated total RNA was combined with 2 μ L of random decamers and water to make a total of 12 μ L. The mixture was incubated at 75°C for 3 minutes in a thermocycler to denature the RNA, then quick-chilled on ice to prevent snap-back. The mixture was then mixed with 0.5 μ L RNase inhibitor, 2 μ L 10X RT-buffer, 4 μ L dNTP. For all +RT tubes, 1 μ L of MMLV reverse transcriptase was used. Tubes without reverse transcriptase were supplemented with 1 μ L of water. The cycle parameters were as follows: tubes were incubated at 43°C for one hour to reverse transcribe the RNA templates, and then the temperature was increased to 92°C for a duration of 10 minutes to denature the reverse transcriptase. The samples remained at 4°C until they were removed from the thermocycler.

Quantitative Real-Time Polymerase Chain Reaction

To obtain a standard curve to validate primer efficiencies, cDNA samples were serially diluted as follows: 1/1, 1/4, 1/16, and 1/64 in nuclease-free water. Two AChR subunit genes were amplified: $\alpha 4$, $\beta 2$, plus GAPDH as the endogenous control. A master mix for each gene was made containing 12.5 μL of SybrGreen (BioRad), 2 μL of the 10 μM sense and antisense primer buffer solution, and 5.5 μL of nuclease-free water (Ambion) (for each well). The total volume of each master mix was dependent upon the number of wells per gene used for the PCR reaction. The primer solution added to the master mix for each gene was diluted to a concentration of 10 μM from the initial 200 μM stock solution by adding 5 μL of the forward primer, 5 μL of the reverse primer, and 90 μL of nuclease-free water. Each well of a 96-well plate contained 5 μL of the respective cDNA template to which 20 μL of respective master mix were added. PCR reactions were performed in an Applied Biosystems 7500 real-time PCR machine for 40 cycles. The parameters for the 40 cycles were as follows: 95°C for 2 minutes, then 50°C for 10 minutes, and 60°C for 1 minute. Upon completion of the standard curve experiment, an optimal dilution (usually 1:16) was chosen where a sufficient quantity of gene expression was observed.

This protocol was repeated for both dose response and time course experiments. However, for the 100 μM nicotine timed response experiment, a 1/5 dilution of cDNA template was used instead of 1/16 due to low RNA quantities.

RESULTS

Cell Morphology

Photographs were taken of the H69 and H460 cells during nicotine treatment at a magnification of 80X. Figures 8A and 8B show untreated and treated (100 μ M nicotine) H460 adherent cells, respectively, at Day 3 during the 4 day time course of nicotine treatment. Figures 9A and 9B show untreated and treated (100 μ M nicotine) H69 suspension cells, respectively, at Day 3 during the 4 day time course of nicotine treatment. Cell morphology did not appear to change during nicotine treatment. All photographs were arbitrarily chosen as representative samples of cell morphology during nicotine treatment.

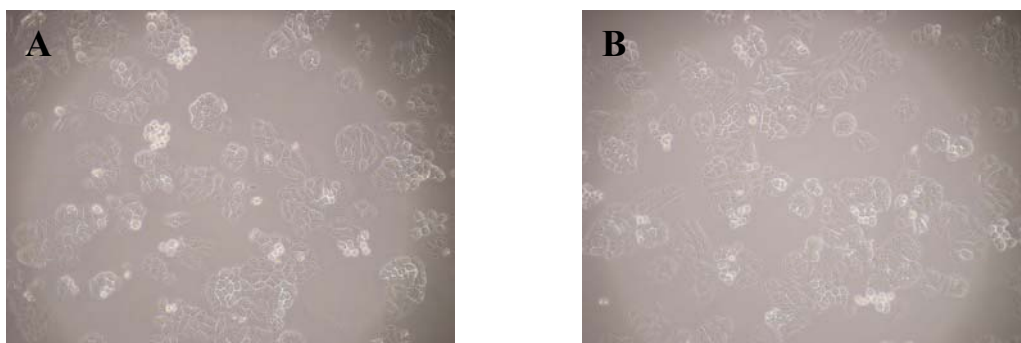


Figure 8: Photographs of the H460 Cells During the Nicotine Time-Course Study. A) A photograph of the untreated control H460 cells on day 3; B) A photograph of the H460 cells treated with 100 μ M nicotine on day 3. Photographs are at 80X magnification.

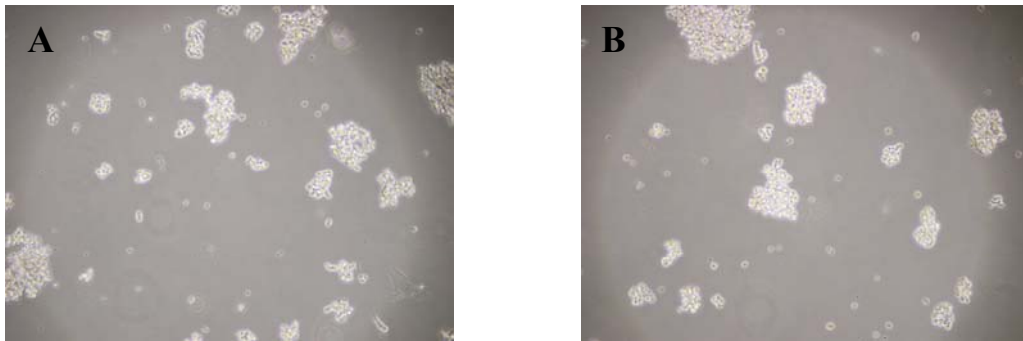


Figure 9: Photographs of the H69 Cells During the Nicotine Time-Course Study. A) A photograph of the untreated control H69 cells on day 3; B) A photograph of the H69 cells treated with 100 μM nicotine on day 3. Photographs are at 80X magnification.

Primer Location and Length

Primers were designed for three target genes (the $\alpha 4$, $\alpha 7$, and $\beta 2$ nAChR subunit genes) and one endogenous control [the glyceraldehydes-3-phosphate dehydrogenase (GAPDH) gene]. Each primer set flanked an intronic sequence to ensure the absence of genomic contamination, details of which can be found in the methods section of this report. The schematic drawing in Figure 10 illustrates the location of the $\alpha 4$ -specific primers. The forward primer spanned exon 2, and the reverse primer spanned exon 3. The amplicon product resulting from these primers had a length of 134 base pairs (bp).

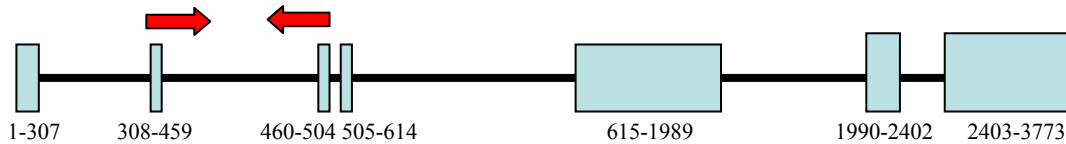


Figure 10: Primer Location for the $\alpha 4$ Gene. This diagram shows the exon/intron structure of the $\alpha 4$ gene. The blue boxes represent exons while the black lines represent introns. The red arrows illustrate the forward (right-pointing) and reverse (left-pointing) primers.

The schematic drawing in Figure 11 shows the location of the $\beta 2$ -specific primers. The forward primer spanned exon 2 and the reverse primer spanned exon 3. The amplicon product resulting from these primers had a length of 63 bp.

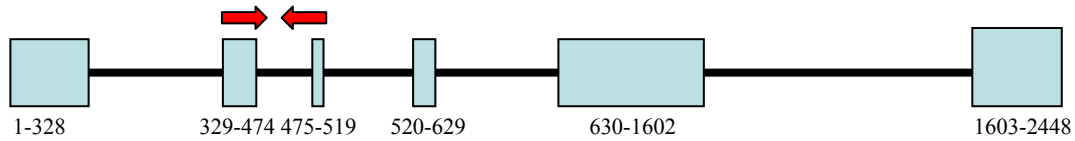


Figure 11: Primer Location for the $\beta 2$ Gene. A schematic drawing showing the exon/intron structure of the $\beta 2$ gene. The blue boxes represent exons while the black lines represent introns. The red arrows illustrate the forward (right-pointing) and reverse (left-pointing) primers.

The schematic drawing in Figure 12 illustrates the location of the $\alpha 7$ -specific primers. The forward primer spanned exon 5 and the reverse primer spanned exon 6. The amplicon resulting from these primers had a length of 77 bp.

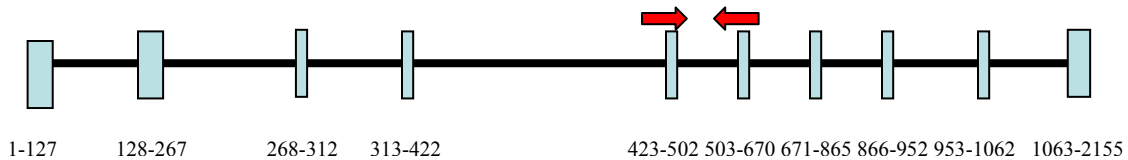


Figure 12: Primer Location for the $\alpha 7$ Gene. A schematic drawing showing the the exon/intron structure of the $\alpha 7$ gene. The blue boxes represent exons while the black lines represent introns. The red arrows illustrate the forward (right-pointing) and reverse (left-pointing) primers.

Primer Specificity

Primer specificity was determined in both the H69 and H460 cell lines prior to nicotine treatment (Figures 13 and 14). This was necessary to validate the primers and to determine their efficiencies. The cDNA template of each cell line was serially diluted (1:1, 1:4, 1:16, 1:64) in order to create a standard curve, which is essential as a first step

towards determining primer efficiencies. These serial dilutions were also created to determine the optimal dilution for all subsequent experiments.

The specificity of each set of primers in the H460 cells is shown in Figure 13. To revisit what is seen in the real-time PCR data, an amplification plot helps to determine what products are amplified by the primers. A dissociation curve assists in establishing primer specificity. If a primer set is specific, only one peak should be observed at the correct melting temperature in the dissociation curve. Additionally, amplification should only be seen in the samples that contained reverse transcriptase in the RT-PCR experiment, and not within those samples that did not contain reverse transcriptase (-RT).

$\alpha 4$ $\alpha 7$ $\beta 2$

GAPDH

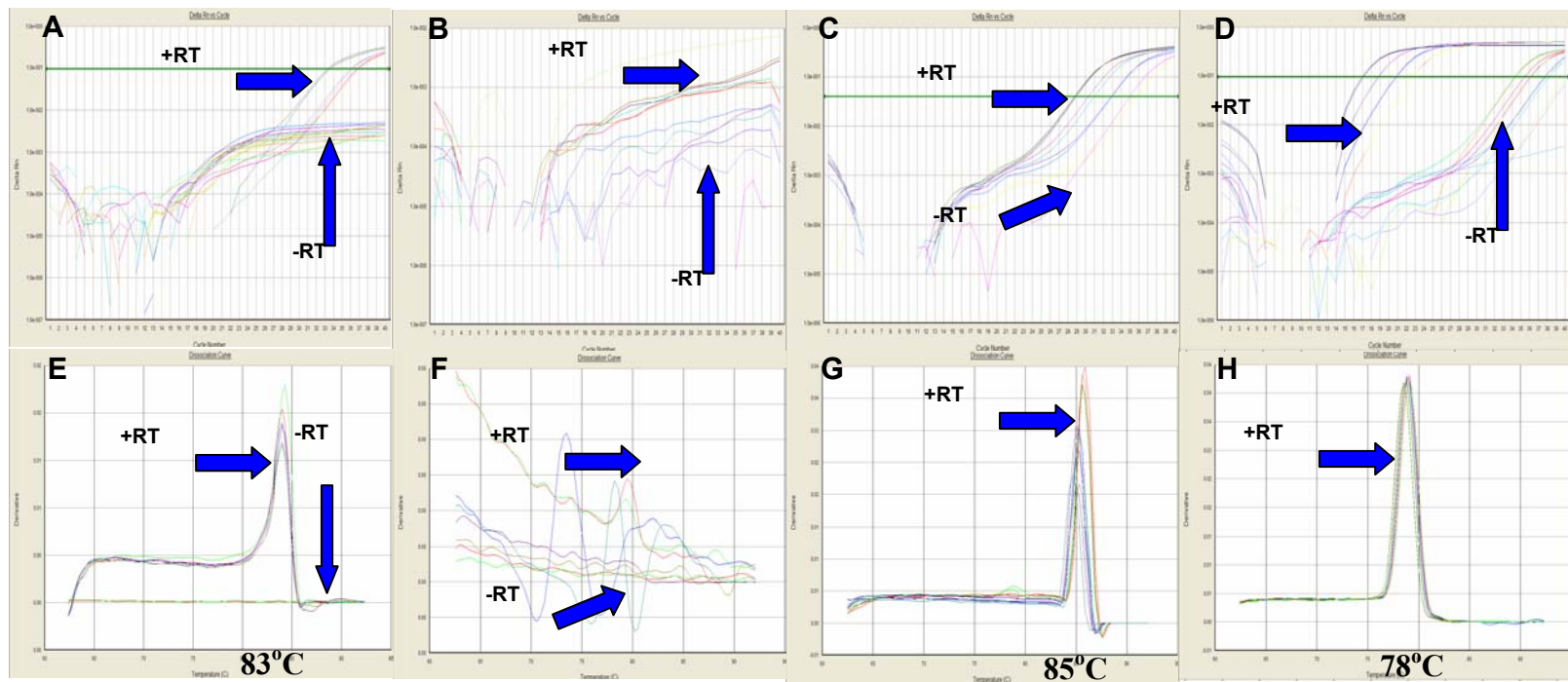


Figure 13: Primer Specificity in the H460 Cell Line. The x-axis represents the melting temperatures (relevant melting temperatures enlarged) while the y-axis represents the ΔRn (derivative of fluorescence). **A-D:** Amplification plots of the $\alpha 4$, $\alpha 7$, $\beta 2$, and GAPDH genes by their respective primers in the H460 cell line. Each subunit cDNA template was serially diluted 1:1, 1:4, 1:16, 1:64, each of which is portrayed by the specific lines in the amplification plots. Note the amplification of nonspecific products in the $\alpha 7$ graph. **E-H:** Dissociation curves of the $\alpha 4$, $\alpha 7$, and $\beta 2$ genes by their respective primers in the H460 cell line. Again, note the non-specificity of the $\alpha 7$ primers. Also note that the $\beta 2$ primers are amplifying a product at a melting temperature of 85°C rather than the predicted amplicon melting temperature of 80°C.

$\alpha 4$ $\alpha 7$ $\beta 2$

GAPDH

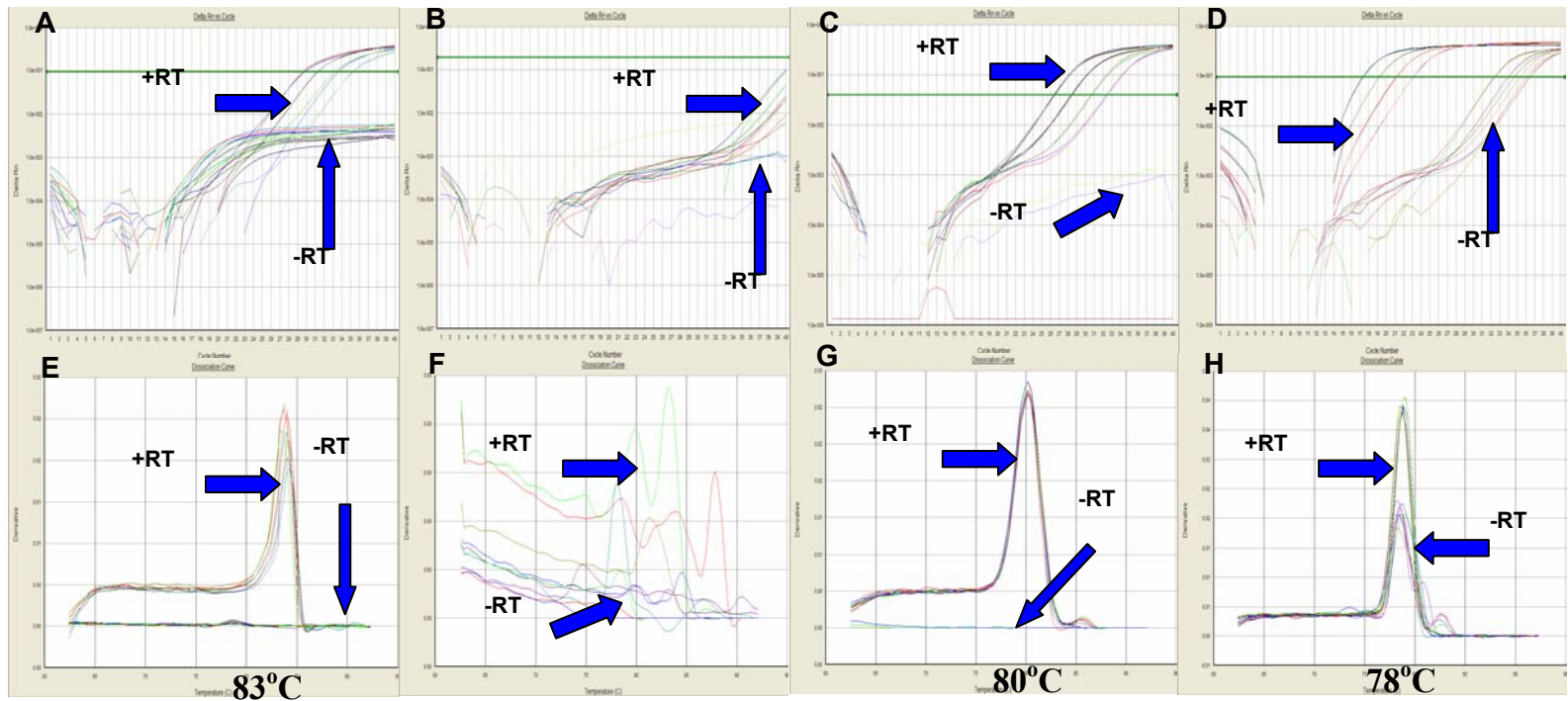


Figure 14: Primer Specificity in the H69 Cell Line. The x-axis represents the melting temperatures (relevant melting temperatures enlarged) while the y-axis represents the ΔRn (derivative of fluorescence). **A-D:** Amplification plots of the $\alpha 4$, $\alpha 7$, $\beta 2$, and GAPDH genes by their respective primers in the H69 cell line. Each subunit cDNA was serially diluted 1:1, 1:4, 1:16, 1:64, each of which is portrayed by the specific lines in the amplification plots. **E-H:** Dissociation curves of the $\alpha 4$, $\alpha 7$, and $\beta 2$ genes by their respective primers in the H69 cell line. Note the non-specificity of the $\alpha 7$ primers. Also note that the $\beta 2$ primers are amplifying the correct predicted product at a melting temperature of 80°C as compared to the incorrect amplicon at 85°C in the H460 cell line.

The $\alpha 4$ Primers are Specific in the H69 and H460 Cell Lines

In our preliminary experiments, it was discovered that the $\alpha 4$ primers are specific in both the H69 and H460 cells, shown by the absence of amplification in the -RT wells (Figures 13A and 14A, respectively), as well as the single peak at the correct melting

temperature (84°C) in the dissociation curves (Figures 13E and 14E, respectively). One important point to mention is the observation of lower expression of this subunit within both the H69 and H460 cell lines as compared to either the $\beta 2$ or GAPDH amplification shown in Figure 13. This can be stated because of the high cycle number at which the $\alpha 4$ target amplicon is first detectable (cycle number 30). It was determined that the 1:16 dilution was sufficient for the detection and analysis of this nAChR subunit gene.

The $\alpha 7$ Primers are Not Specific in the H69 and H460 Cell Lines

Issues were encountered with the $\alpha 7$ primers in both cell lines as can be seen in the non-specificity of the target gene shown in the H460 cells (Figures 13B and F) and in the H69 cells (Figures 14B and F). Not only was there an absence of a single peak in the dissociation curves, but the amplification in either cell line did not reach a threshold value where all of the dilutions were amplified at the same rate. These primers were redesigned in an attempt to obtain primers specific for the gene of interest, however no improvement in the results were observed with the second set of primers. Therefore, this nAChR subunit was neither further pursued nor was the optimal dilution of cDNA determined as it was unlikely, due to time constraints, that a third set of primers could be designed.

The $\beta 2$ Primers are Not Specific in the H69 and H460 Cell Lines

In addition to the $\alpha 7$ primers, the $\beta 2$ primers also lacked specificity, although to a lesser extent in both the H460 and H69 cell lines (Figures 13C, G, and 14C, G, respectively). Specifically, the correct amplicon in the H69 cells was amplified (melting

temperature of 80°C determined by PrimerExpress[®] software), however an incorrect target was amplified in the H460 cells (melting temperature of 85°C). Although the primers amplified the correct target in the H69 cells, there is a slight peak at 85°C to the right of the main target peak in the dissociation curve (Figure 14G), indicative of amplification of a non-specific product.

As described above, the $\beta 2$ primers had a small amount of non-specific amplification in the H69 cells. However, this non-specific amplification was much higher in the H460 cells and the $\beta 2$ primers actually favored this non-specific target over the $\beta 2$ gene. Figure 13G shows how the non-specific amplification at 85°C is higher than the target amplicon at 80°C. To further analyze this non-specificity and compare the size of the non-specific product to the predicted size of the target amplicon, gel electrophoresis was performed on a 1.7% agarose-TBE gel. Figure 15 shows the separation of the $\beta 2$ amplicon products of the H69 and H460 cells. If each cell sample has one band corresponding to the specific target, the size should be approximately 63bp. However, as seen in Figure 16, the H460 cell line has a highly concentrated band of approximately 100 bp corresponding to a non-specific amplicon. Although the non-specific amplicon in the H69 cell line cannot be detected in this gel, it should be noted that the slight peak in the dissociation curve at the incorrect temperature of 85°C (Figure 14G) does provide evidence of non-specific amplification.

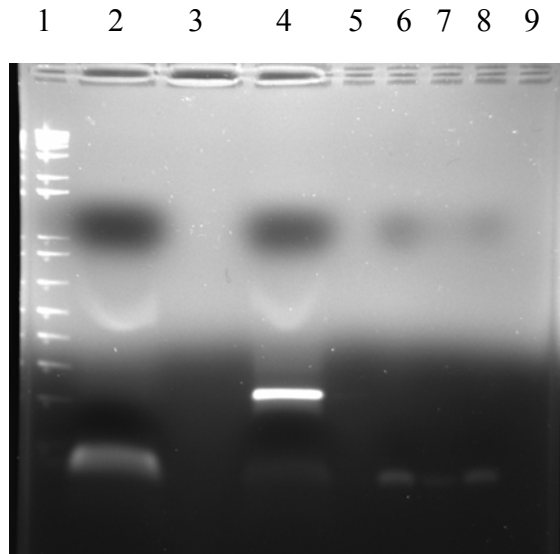


Figure 15: Separation of $\beta 2$ Amplicon Products in Both H69 and H460 Cell Lines on 1.7% agarose/TBE. Lane 1: 1kb marker; lane 2: H69 sample; lane 4: H460 sample; lanes 6 & 8: positive control; lanes 3, 5, 7, & 9: empty. Note that the amplicon within the H69 cell line corresponds to the approximate size of the positive control, but the amplicon in the H460 cell line is entirely different.

In addition to the speculation of non-specific amplification by the $\beta 2$ primers, the possible presence of contamination was also considered. However, contamination was discarded as a possibility since the same reagents were used for each primer set, and no contamination was evident in any previous or future real-time PCR experiment of the nAChR $\alpha 4$ subunit. It was then hypothesized that perhaps the $\beta 2$ primer stock was contaminated, as this is the only difference between each nAChR subunit's set of samples in a real-time PCR experiment. However, after reordering new primers, the 'contamination' was still present. Therefore, it was reaffirmed that the amplification within the $\beta 2$ -RT samples was due to non-specific amplification. Thus, after all of these aforementioned analyses, the $\beta 2$ primers were not used in subsequent experiments as their efficiency would be decreased due to competition between the correct and incorrect targets within this cell line, thereby negating their use for relative gene expression

quantification. In conclusion, the $\beta 2$ subunit was not further studied due to time constraints.

The GAPDH Primers are Specific in the H69 and H460 Cell Lines

The GAPDH primers were specific in both the H460 and H69 cell lines (Figure 13D, H, and 14D, H, respectively). However, while the GAPDH samples did exhibit non-specific amplification in –RT samples, these primers were believed to be specific for the following reasons. To begin, there is only one peak present in the dissociation curves of both H460 and H69 cell lines in the +RT samples, which is very important (Figures 13H and 14H, respectively). Additionally, despite the fact that the non-specific amplification did occur with the GAPDH primers in the –RT samples, it was not detectable until cycle number 35. This is in comparison to the amplification of the correct target gene, detectable at cycle number 17. It is important to note that a typical RT-PCR reaction is not extended past the 30th cycle. In a real-time PCR experiment however, the machine is automatically set to carry out 40 cycles. As an example, since the $\alpha 4$ subunit gene is present in such a low concentration within both cell lines, it was not detectable until about cycle number 30 (Figures 13A and 14A). Therefore, the PCR experiment would have to be run past cycle number 30 in order to observe the $\alpha 4$ gene expression. However, because the specific target of the GAPDH primers is in such high concentration within both cell lines, it was detectable at cycle 17 and theoretically, the PCR reaction would not need to run past cycle 30. Therefore, the non-specific amplification observed after cycle 30 was considered negligible and concluded to be insignificant as it was not observed until the later phase of the PCR experiment.

Another reason that this non-specific amplification was concluded to be negligible in the GAPDH samples was due to the sensitivity of real-time PCR. Because of this sensitivity, any non-specific target could theoretically be amplified even at low dilutions. Since RNA was not reverse transcribed in the -RT samples, the GAPDH primers theoretically had nothing available in the real-time PCR experiment to amplify. Therefore, it is highly probable that they amplified anything within the sample wells present in an extremely low concentration. This could be considered to be contamination; however, because the primers are so specific for their target gene, and thus primer efficiency would not be decreased, GAPDH was used as the endogenous control for subsequent experiments. In summary, the GAPDH primers were used for additional experiments as they satisfied the requirement of specificity in these preliminary experiments. Additionally, the 1:16 dilution was also determined to be a sufficient dilution to use in subsequent experiments.

The $\alpha 4$ Subunit is Valid for Relative Gene Expression Quantification Using the $\Delta\Delta C_t$

Method

Establishing primer specificity is the first step in determining whether gene expression can be quantified using the $\Delta\Delta C_t$ method, which is a relative method of quantification (Livak and Schmittgen, 2001). Once the primers are established to be specific to the targets of interest, the next step is determining primer efficiencies between the target gene(s) and the endogenous control. This is an essential aspect of relative quantification since this approach describes a change in target gene expression relative to a reference group (Livak and Schmittgen, 2001). Therefore, determining the efficiencies

of the $\alpha 4$ and GAPDH primers was an essential analysis prior to quantification in order to validate the use of the $\Delta\Delta C_t$ method.

Amplification efficiency is measured as the ability of primers specific for distinct genes (in our case, $\alpha 4$ and GAPDH) to amplify their target genes at the same rate (Livak and Schmittgen, 2001). This measurement is established by first producing a standard curve for each set of primers, using serial dilutions, and then determining how the cycle number changes with each dilution. To begin this process, the average cycle number for each cDNA dilution, performed in triplicate, must be calculated for each target gene. Once these averages are established, the average cycle number for the endogenous control is subtracted from each target gene to determine the change in cycle number compared to the control, or ΔC_t . The log of the cDNA dilutions are then plotted on a graph versus the ΔC_t values at each dilution. If the absolute value of the slope is close to zero, then the efficiencies of the target and endogenous control primers are considered to be similar and the $\Delta\Delta C_t$ method is validated for use (Livak and Schmittgen, 2001).

The $\alpha 4$ and GAPDH efficiencies were analyzed using the aforementioned methods. Linear regression analysis of $\alpha 4$ primer efficiency is shown in Figure 16. Because the absolute value of the slope of the line, 0.123, the $\alpha 4$ primers were able to be used for quantitative gene expression analysis.

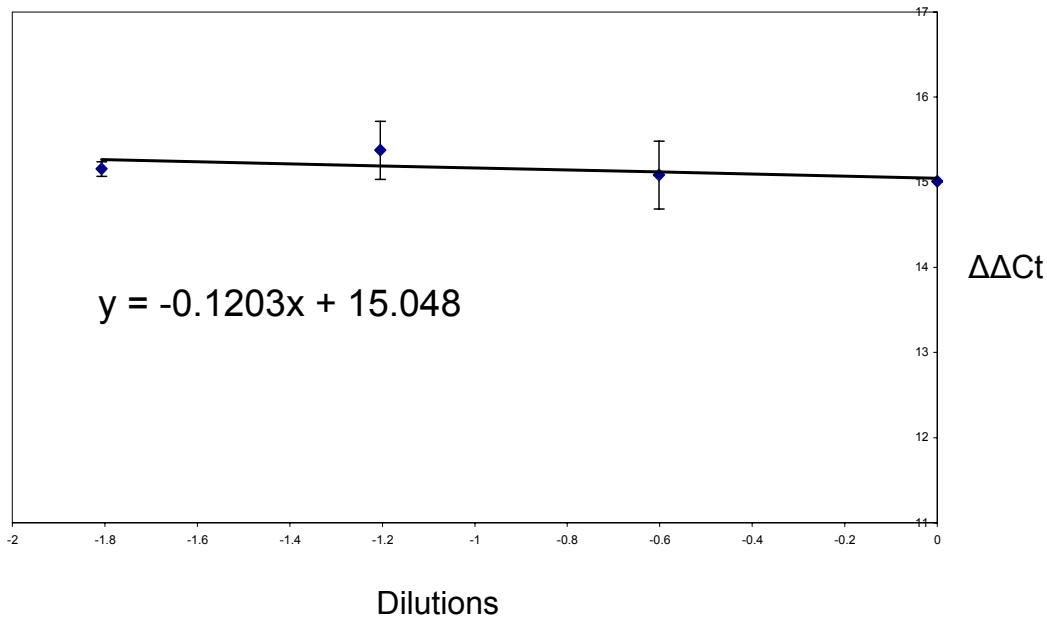


Figure 16: Linear Regression Analysis of $\alpha 4$ Primer Efficiency. $\alpha 4$ primer efficiency was compared against GAPDH primer efficiency in order to validate the $\alpha 4$ primers for relative gene expression quantification by the $\Delta\Delta C_t$ method. The absolute value of the slope of the line, 0.1203, was within the boundaries for primer validation.

The nAChR $\alpha 4$ Subunit Gene is Expressed 4-fold Higher in the H69 Cell Line Compared to the H460 Cell Line.

Immediately after validating the use of the $\alpha 4$ primers, basal gene expression levels were quantified in both the H69 and H460 cell lines using the $\Delta\Delta C_t$ method. It was found that this subunit, although already expressed in low concentrations (shown by the high cycle number [30] necessary to detect amplification in Figures 13A and 14A) within both the H69 and H460 cell lines, was expressed at a 4-fold lower level within the H460 cells as compared to the H69 cells (Figure 17). This relative gene expression analysis using the $\Delta\Delta C_t$ method was calculated by a series of equations described in detail by Livak and Schmittgen (2001).

To provide some detail, the average cycle number (C_t) of each target gene is calculated and normalized against the endogenous control in order to account for any variance in the initial starting RNA concentrations (ΔC_t) (Livak and Schmittgen, 2001). Standard deviations are calculated from triplicate samples of each gene. The ΔC_t is then calculated as described above in the previous section. Because the expression of the $\alpha 4$ subunit gene was compared between cell lines in this study, one cell line had to be chosen as a reference point with which to compare any differences in expression of the $\alpha 4$ subunit gene. Therefore, to begin this calculation, the H460 cell line was arbitrarily chosen as the calibrator. Next, the $\Delta \Delta C_t$ calculation is performed. To do so, the ΔC_t of the $\alpha 4$ subunit in the H460 cell line was subtracted from itself to obtain a value of zero (again, this was done in order to use the H460 cell line as a calibrator). Then the ΔC_t for $\alpha 4$ subunit gene expression in the H460 cell line was subtracted from the $\alpha 4$ subunit gene expression in the H69 cell line. This was done to obtain the $\Delta \Delta C_t$ value for the H69 cells. Finally, the $\Delta \Delta C_t$ values for both the H69 and H460 cell lines were used to calculate the normalized relative gene expression in the equation $2^{-\Delta \Delta C_t}$. These values were then plotted on a bar chart to visually represent the difference in gene expression between the two cell lines, shown in Figure 17.

As stated previously, the H69 cell line was characterized by a 4-fold higher level in $\alpha 4$ subunit gene expression as compared to the H460 cell line. The H69 cell line was chosen for study as it appeared to be a stronger candidate than the H460 cells after evaluation of primer non-specificity and low $\alpha 4$ subunit gene expression.

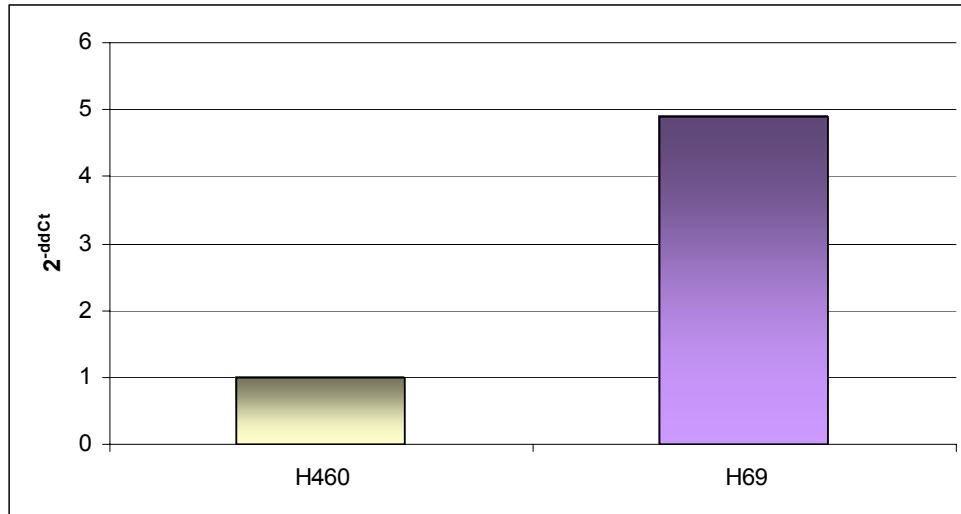


Figure 17: Relative Quantitative Analysis of $\alpha 4$ Gene Expression in the H460 and H69 Cell Lines. This graph shows the 4-fold higher level of $\alpha 4$ gene expression in the H69 cell line as compared to the H460 cell line determined by the $2^{-\Delta\Delta Ct}$ calculation.

Nicotine Dose Response Study

To study the effects of nicotine on nAChR subunit gene expression in the H69 cell line, a dose response experiment was an essential first step towards determining the optimal nicotine concentration to treat the cells in further experiments. This dose response experiment tested an exponential range of nicotine concentrations: 1 μM , 10 μM , and 100 μM over a period of seven days. These concentrations were chosen based on previous studies by other laboratories using a variety of all lines (Peng *et al*, 1997; Pidoplichko *et al*, 1997). A concentration of 1000 μM was not studied as it is not physiologically relevant to the blood nicotine levels experienced by smokers (Pidoplichko *et al*, 1997).

The optimal dose of nicotine is chosen by determining the concentration at which gene expression has changed the most in comparison to the untreated control. A

significant change in expression is visually established by a difference of two or more cycles between the untreated control and the target of interest. Since $\alpha 4$ subunit gene expression differed by two cycle numbers in response to 100 μM nicotine, it was determined that this concentration affected gene expression the most (Figure 18A). A visual analysis was the only tool available after this study was performed because mathematical analysis tools were not available at the time. However, towards the end of this project, when these tools were available, reanalysis of these data unexpectedly showed that 10 μM nicotine had actually increased gene expression the most as compared to an untreated control. Therefore, while 100 μM nicotine was the concentration used for all subsequent nicotine treatment experiments in our project, it is important to consider using 10 μM nicotine treatment in future studies.

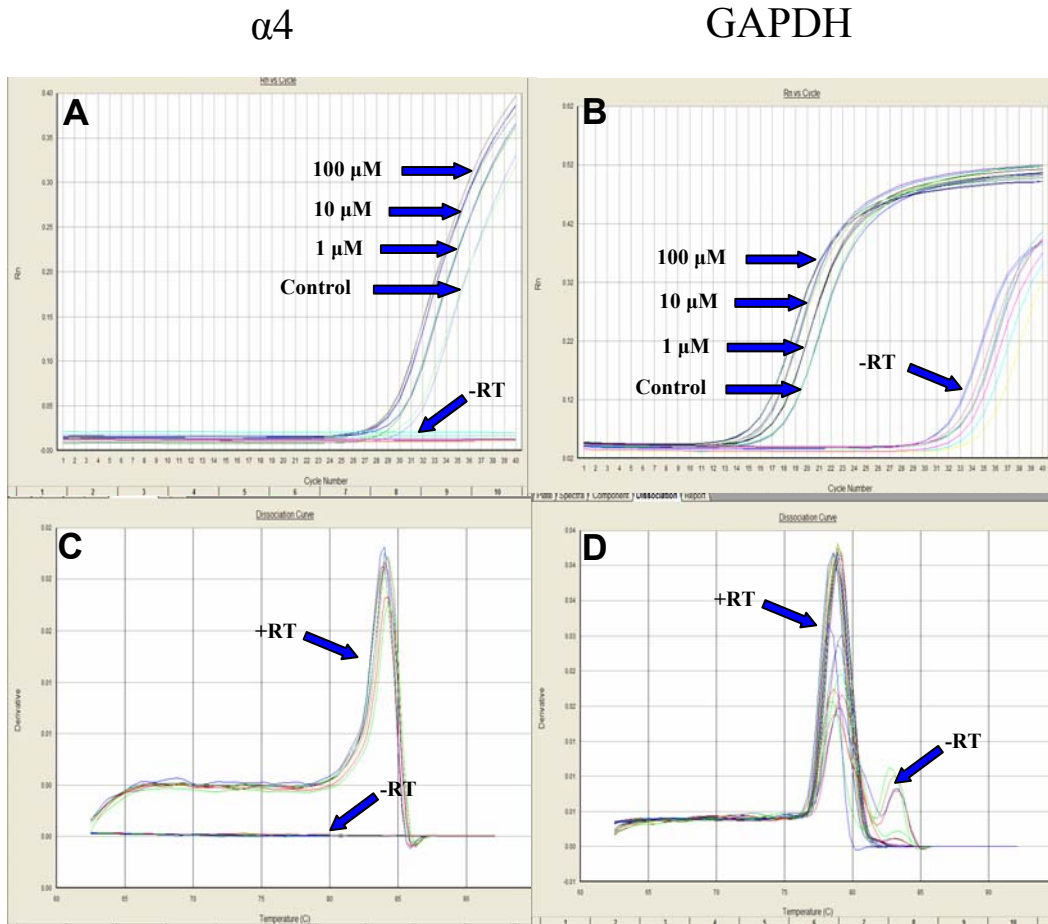


Figure 18: Nicotine Dose Response Experiment of the H69 Cell Line. A-B. Amplification plots for the H69 cells of the $\alpha 4$ and GAPDH genes, respectively. C-D. Dissociation curves for the H69 cells of the $\alpha 4$ and GAPDH genes, respectively. H69 cells were treated with 1 μM , 10 μM , or 100 μM nicotine over a period of seven days to determine the optimal dose of nicotine to use in subsequent experiments.

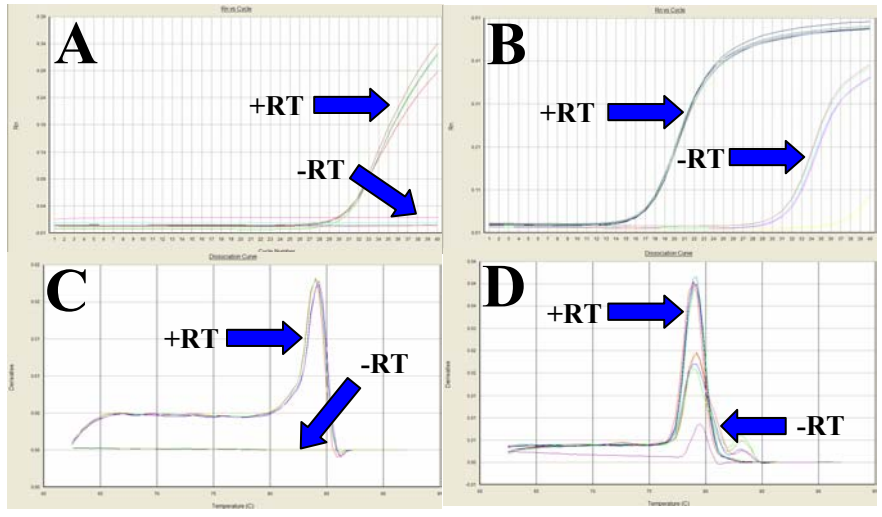
Nicotine Time-Course Study Using the H69 Cell Line

In order to study the short-term effects that treatment of H69 cells with 100 μM nicotine has on nAChR subunit gene expression, a time-course experiment was performed. Samples were harvested at time zero hours, 24 hours, and four days. Analysis showed that at zero hours and four days, no increase in gene expression compared to the untreated control was observed (Figures 19A-B, K-L). However, at 24 hours, there was a significant increase in gene expression compared to the untreated controls, characterized

by a difference of more than two cycle numbers (Figures 19G-I). However, in addition to this, GAPDH gene expression also changed significantly with nicotine treatment at 24 hours. Therefore, no relative quantitative analyses can be performed on the expression of the $\alpha 4$ subunit gene during this time-course study. Since the validity of using an endogenous control during real-time PCR experiments is attributed to a housekeeping gene's hypothetical stable expression, changes in control gene expression are not acceptable if quantification is to be performed. If control gene expression does change during treatment, a different control must be tested. Therefore, because GAPDH gene expression increased with nicotine treatment during the time-course experiment, quantitative data analysis could not be performed. However, despite this fact, it was possible to make some qualitative assumptions addressed in the Discussion section of this report. Due to time constraints, it was not possible to choose an alternative endogenous control, design primers, and repeat all of the previously undertaken experiments.

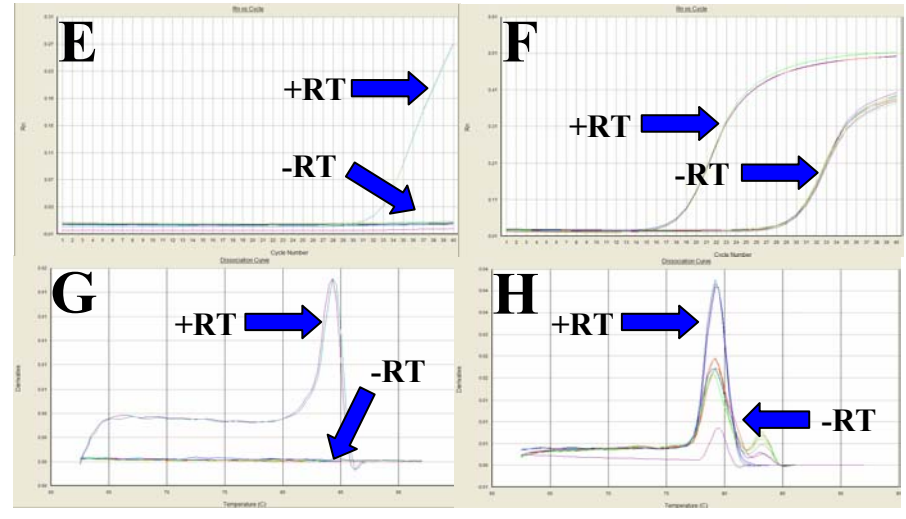
$\alpha 4$

GAPDH



$\alpha 4$

GAPDH



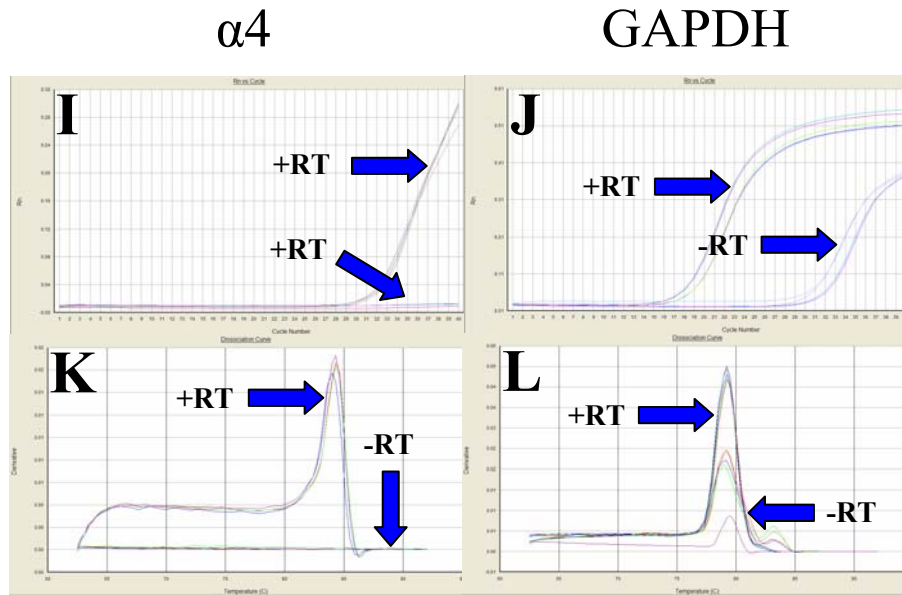


Figure 19: Time-Course Experiment With 100 μ M Nicotine Treatment of the H69 Cell Line. These graphs show the amplification plots (upper panels in each set) and dissociation curves (lower panels in each set) of the time-course experiment of 100 μ M nicotine treatment of H69 cells on expression of the nAChR α 4 subunit .

A-B. Zero time point amplification plots of the α 4 and GAPDH genes, respectively.

C-D. Zero time point dissociation curves of the α 4 and GAPDH genes, respectively.

E-F. 24 hour time point amplification plots of the α 4 and GAPDH genes, respectively.

G-H. 24 hour time point dissociation curves of the α 4 and GAPDH genes, respectively.

I-J. Four day time point amplification plots of the α 4 and GAPDH genes, respectively.

K-L. Four day time point dissociation curves of the α 4 and GAPDH genes, respectively.

DISCUSSION

The purpose of this study was to analyze the effects of nicotine treatment on the expression of nicotinic acetylcholine receptor (AChRs) genes in the H69 and H460 human lung carcinoma cell lines. The cells were treated using a range of nicotine concentrations to determine the optimal dose required to observe an effect on gene expression.

To begin this project, efficient primers were necessary to amplify the target genes within these cell lines. We designed primer sets for the $\alpha 4$, $\alpha 7$, and $\beta 2$ nAChR subunit genes, and the housekeeping gene GAPDH. While the $\alpha 4$ primers were efficient in amplifying the correct target in both cell lines, the $\alpha 7$ primers were non-specific for their target gene in both the H69 and H460 cell lines as can be seen in Figures 13 and 14. Since non-specific amplification decreases the efficiency of the primers to amplify the target gene at a hypothetical 100%, the $\alpha 7$ subunit had to be discredited for quantitative analysis and further experiments.

The $\beta 2$ primers were specific for the target gene in the H69 cell line; however, they were not specific in the H460 cell line. This was determined by the proposed amplicon melting temperature provided by PrimerExpress[®]. The correct melting temperature for the $\beta 2$ amplicon was 80°C, which was observed in the H69 cell line. However, in the H460 cell line, the amplicon melting temperature was observed at 85°C. Despite the first assumptions that the $\beta 2$ primers were specific for their target in the H69 cell line, further analysis proved that these primers were also amplifying non-specific products in H69 cells. Therefore, the $\beta 2$ primers were also discredited for quantitative

analysis and further experiments since non-specific amplification decreases primer efficiency.

Amplification of the $\alpha 4$ subunit gene by its respective primers was specific, however, expression was low in both cell lines. Since the $\alpha 4$ primers were specific in both cell lines, their efficiency (compared to that of the endogenous control GAPDH) was analyzed and showed that they were valid for quantifying gene expression using the $\Delta\Delta C_t$ method. Quantification analysis using this method established that the $\alpha 4$ subunit gene is expressed at a 5-fold lower level in the H460 cell line as compared to the H69 cell line (Figure 17). Therefore, all of the aforementioned results led us to conclude that with the limited time available, the H69 cell line was a much stronger candidate for nicotine treatment studies.

A dose-response experiment was then performed on the H69 cell line over a period of seven days in order to determine the optimal nicotine concentration to treat cells in subsequent experiments. After data analysis, it was observed that 100 μM nicotine increased the nAChR subunit gene expression the most compared to the untreated controls. Therefore, this concentration was used for all subsequent experiments. However, upon reanalysis of these data at a later time point, it was unexpectedly discovered that the 10 μM nicotine concentration had actually produced the greatest change in $\alpha 4$ subunit gene expression, an important point for future experiments.

A time-course experiment was then performed using 100 μM nicotine in order to study the short-term effects of nicotine treatment on $\alpha 4$ nAChR subunit gene expression in the H69 cell line. The purpose of this experiment was to further analyze exactly when the increase in subunit gene expression occurs in order to further provide information on

the gene expression of nAChRs, and the mechanism behind nicotine addiction. After data analysis, the most prominent change in $\alpha 4$ gene expression was an increase at 24 hours. This time-point is of great interest since $\alpha 4$ subunit gene expression in the untreated control was undetectable compared to the treated samples. Furthermore, amplification of the $\alpha 4$ subunit in the GAPDH and treated samples at the 0 and 4 day time points were detectable, but no change in gene expression was detected in any of these samples (Figures 19A-L).

Although the expression of the GAPDH gene was not previously determined to change with nicotine treatment during the dose-response experiment, it unfortunately increased compared to the untreated controls during the time-course study, specifically at 24 hours (Fig 13D-H). Moreover, throughout each real-time PCR, the GAPDH samples that were not reverse transcribed (-RT) were observed to have amplification. This led us to the conclusion that these samples were either contaminated, or the primers were non-specific. To elaborate, it is possible that contamination was not an issue as the same reagents were used for each cDNA sample, and amplification was never observed in any of the -RT $\alpha 4$ samples. Therefore, non-specific amplification by the GAPDH primers may have been the issue at hand. However, this cannot be proven since the 'no template controls' (NTC), where no cDNA template was present, of the GAPDH samples also had amplification. The oddity in this observation is that the $\alpha 4$ NTC samples never had amplification. Therefore, if it was contamination, it should have been present in these samples throughout each experiment. In conclusion, it is difficult to confidently state what phenomenon was occurring. It may also be possible that nicotine treatment of these cells indeed upregulates GAPDH expression, and that GAPDH can no longer be

considered a true “housekeeping” gene. GAPDH has been shown to have functions other than housekeeping glucose metabolism (Tisdale, 2002).

In summary, due to the unexpected results throughout each experiment, the following are suggested recommendations. First and foremost, a new endogenous control must be chosen, validated, and observed for changes in gene expression during nicotine treatment. Since a new endogenous control is necessary, all previous experiments must be repeated. In addition, new $\beta 2$ and $\alpha 7$ primers must be designed such that they are specific for their target gene in both cell lines.

Due to the unexpected result after data analysis that 10 μM nicotine stimulated the greatest change in $\alpha 4$ subunit gene expression, this phenomenon should be further evaluated. Furthermore, the time-course experiment should also be repeated in order to verify the increase in gene expression observed in the $\alpha 4$ subunit at 24 hours. If these data are reproducible, additional nicotine treatment studies should be performed where samples are taken on an hourly basis to determine precisely the length of time required to see this change in gene expression.

The purpose of this project was to quantify gene expression levels of nAChRs subunits after short-term and long-term nicotine treatment. This study is relevant in providing additional information regarding the molecular mechanisms behind nicotine addiction and cancer. It is essential to use techniques such as real-time PCR to provide quantitative analysis for future research.

REFERENCES

American Cancer Society (2005) Facts and Figures. *Statistics for 2005*. Found on April 3, 2005 at: <http://www.cancer.org/docroot/home/index.asp>

Benhammou K *et al* (2000) [³H] Nicotine binding in the peripheral blood cells of smokers is correlated with the number of cigarettes smoked per day. *Neuropharmacology* 39: 2818-2829.

Benwell ME, Anderson JM, and Balfour DJ (1988) Evidence that Tobacco Smoking Increases the Density of (-)-[³H]nicotine Binding Sites in Human Brain. *Journal of Neurochemistry*, 50(4): 1243-1247.

Cattaneo MG *et al* (1993) Nicotine Stimulates a Serotonergic Autocrine Loop in Human Small-Cell Lung Carcinoma. *Cancer Research*, 53: 5566-5568.

Dajas-Bailador F and Wonnacott S (2004) Nicotinic Acetylcholine Receptors and the regulation of Neuronal Signaling. *TRENDS in Pharmacological Sciences*, 25(6): 317-324.

Dani JA, Ji D and Zhou FM (2001) Synaptic Plasticity and Nicotine Addiction. *Neuron*, 31: 349-352.

Dart MJ *et al* (2000) Structural Aspects of High Affinity Ligands For The alpha 4 beta 2 Neuronal Nicotinic Receptor. *Pharmaceutica acta Helvetiae*, 74:115-123.

Dorak MT (2005) Real-time PCR. *Clinical Medical Sciences*. Found on March 30, 2005 at: <http://dorakmt.tripod.com/genetics/realtime.html>

Institute of Neurosciences (2005) How Drugs Affect Neurotransmitters. Found on March 30, 2005 at: http://www.thebrain.mcgill.ca/flash/i/i_03/i_03_m/i_03_m_par/i_03_m_par_nicotine.html

Jain R and Murkherjee K (2003) Biological Basis of Nicotine Addiction. *Indian Journal of Pharmacology*, 35: 281-289.

Laviolette SR and van der Kooy D (2004) The Neurobiology of Nicotine Addiction: Bridging the Gap from Molecules to Behaviour. *Nature Reviews Neuroscience*, 5: 55-65.

Lechniak D (2002) Quantitative Aspect of Gene Expression Analysis in Mammalian Oocytes and Embryos. *Reproductive Biology*, 2(3): 229-241.

Livak KJ and Schmittgen TD (2001) Analysis of Relative Gene Expression Data Using Real-Time Quantitative PCR and the $2^{-\Delta\Delta C_t}$ Method. *Methods*, 25: 402-408.

- Mai H *et al* (2003) A Functional Role for Nicotine in Bcl2 Phosphorylation and Suppression of Apoptosis. *The Journal of Biological Chemistry*, 278(3): 1886-1891.
- Marks M *et al* (1992) Nicotine Binding and Nicotinic Receptor Subunit RNA After Chronic Nicotine Treatment. *The Journal of Neuroscience*, 12(7): 2765-2784.
- National Institute on Drug Abuse (NIDA) Research Report Series (2001) Nicotine Addiction. *National Institute of Health*, 1-8. Found on March 25, 2005 at: <http://www.nida.nih.gov/researchreports/nicotine/nicotine2.html#what>
- Peng X *et al* (1997) Chronic Nicotine Treatment Up-Regulates $\alpha 3$ and $\alpha 7$ Acetylcholine Receptor Subtypes Expressed by the Human Neuroblastoma Cell Line SH-SY5Y. *Molecular Pharmacology*, 51: 776-784.
- Piccioletto MR *et al* (1998) Acetylcholine Receptors Containing the $\beta 2$ Subunit are Involved in the Reinforcing Properties of Nicotine. *Nature*, 391: 173-177.
- Pidoplichko VI (1997) Nicotine Activates and Desensitizes Midbrain Dopamine Neurons. *Nature*, 390: 401-404.
- Provenzano M *et al* (2001) The Usefulness of Quantitative Real Time PCR in Immunogenetics. *Scientific Communications*, 89-91.
- Schapira M, Abagyan R and Totrov M (2002) Structural Model of Nicotinic Acetylcholine Receptor Isoforms Bound to Acetylcholine and Nicotine. *BMC Structural Biology*, 2(1): 1-8.
- Séguéla P *et al* (1993) Molecular Cloning, Functional Properties, and Distribution of Rat Brain $\alpha 7$: A Nicotinic Cation Channel Highly Permeable to Calcium. *Journal of Neuroscience*, 13(2): 596-604.
- Severance EG *et al* (2004) The $\alpha 7$ Nicotinic Acetylcholine Receptor Subunit Exists in Two Isoforms that Contribute to Functional Ligand-Gated Ion Channels. *Molecular Pharmacology*, 66: 420-429.
- Song P *et al* (2003) Synthesis of Acetylcholine by Lung Cancer. *Life Sciences*, 72: 2159-2168.
- Tisdale EJ (2002) Glyceraldehyde-3-phosphate Dehydrogenase is Phosphorylated by Protein Kinase C α/λ and Plays a Role in Microtubule Dynamics in the Early Secretory Pathway. *Journal of Biological Chemistry*, 277: 3334-3341.
- Trombino S *et al* (2004) $\alpha 7$ -Nicotine Acetylcholine Receptors Affect Growth Regulation of Human Mesothelioma Cells: Role of Mitogen-Activated Protein Kinase Pathway. *Cancer Research*, 64: 135-145.